

Electronic properties of quantum wells in perturbing fields

R. T. Collins, L. Viña,* and W. I. Wang

IBM T. J. Watson Research Center, P. O. Box 218
Yorktown Heights, NY 10598

C. Mailhot

Xerox Webster Research Center, 800 Phillips Road, 0114-41D
Webster, NY 14580

D. L. Smith

Los Alamos National Laboratory
Los Alamos, NM 87545

Abstract

Studies of the response of excitonic transitions in quantum wells to external perturbations have proven useful in understanding the electronic properties of quantum wells. This paper discusses the use of two such perturbations, electric fields and uniaxial stress, in photocurrent and photoluminescence excitation spectroscopy measurements on GaAs/Al_xGa_{1-x}As quantum wells. When an electric field is present in a square quantum well, forbidden excitonic transitions become visible. The excitons also exhibit a Stark shift to lower energies. Since the Stark shifts for different excitons are not the same, it is possible to tune the energy separations between the excitons. By applying electric fields to a 160 Å well, an anticrossing between the excited states of the first heavy hole exciton and the 1s ground state of the first light hole exciton has been observed. The effect of a uniaxial stress on a quantum well is found to depend strongly upon the axis along which the stress is applied. This is in contrast to bulk GaAs. The application of a uniaxial stress to a quantum well can help determine the valence band symmetry of a particular exciton, since heavy and light hole excitons exhibit different energy shifts in a stress. This fact has been used in conjunction with polarization and electric field dependent measurements to identify exciton peaks which arise from mixing between the second heavy and first light hole valence subbands.

Introduction

*Permanent address: Instituto de Ciencia de Materiales. Universidad de Zaragoza -Consejo Superior de Investigaciones Científicas. 50009 Zaragoza, Spain.

The electronic properties of semiconductor quantum wells and superlattices have been a subject of considerable interest. When a quantum well exists in the conduction or valence band of a semiconductor heterostructure, the confining potential gives rise to bound states in the well. Because the carriers are free to move parallel to the well, each bound state becomes a subband and a sequence of subbands is formed. In a superlattice, multiple quantum wells are grown with the confining barriers sufficiently thin that the subbands in adjacent wells couple. In the simplest approximation each of the subbands in a quantum well or superlattice arises from a particular band in the bulk semiconductor from which the wells were made. Thus, the conduction subbands can be viewed as arising from the zone center states of the conduction bands of the bulk materials, and two sequences of valence subbands (one associated with the heavy hole and one with the light hole valence bands of the bulk semiconductor) are present in the well. In reality, the situation is more complicated. In the case of the valence band, considerable mixing between states of heavy and light hole symmetry has been predicted to occur (see for example Ref. 1-4). This mixing is expected to have a large effect on the properties (such as binding energy and oscillator strength) of the excitonic transitions between the valence and conduction band subbands (see for example Ref. 5-8). In the conduction band of a superlattice, the periodic potential introduced by the layers can lead to the presence of subbands which are derived from states at other locations in the Brillouin zone of the bulk materials (such as the X - point).^{9,10} One method for obtaining information about the band structure and associated electronic properties of a quantum well system is to place the well in a perturbing field and study the effect that the perturbation has on the excitonic transitions in the well. Some of the more commonly used perturbations are hydrostatic pressure, magnetic fields, electric fields, and uniaxial stress.

When GaAs and $\text{Al}_x\text{Ga}_{1-x}\text{As}$ are placed under hydrostatic pressure, the Γ -point and X-point conduction band energies shift with respect to one another. Excitation spectroscopy of GaAs/ $\text{Al}_x\text{Ga}_{1-x}\text{As}$ quantum wells and superlattices under hydrostatic pressure has been used to identify conduction subbands which arise from the X-point of the GaAs wells and $\text{Al}_x\text{Ga}_{1-x}\text{As}$ barriers.¹¹ In the process, a measurement of the band offsets between GaAs and $\text{Al}_x\text{Ga}_{1-x}\text{As}$ was obtained. Similar measurements of GaAs/ $\text{Al}_x\text{Ga}_{1-x}\text{As}$ wells in a magnetic field have revealed Landau level structure in the excited state continuum of the excitons.^{12,13} Based on these measurements, binding energies for the excitons have been obtained and compared to the theoretically predicted binding energies. Stark shifts, changes in lifetime, and changes in oscillator strengths have been observed for excitons in the presence of an electric field (see for example ref. 14-18). Recent work on excitons in GaAs/ $\text{Al}_x\text{Ga}_{1-x}\text{As}$ quantum wells under uniaxial stress have shown evidence for the valence band mixing mentioned above.^{19,20} Although these examples do not provide a comprehensive list of the ways in which perturbation studies of quantum wells have been used, they do indicate the power of these techniques in studies of the properties of quantum wells. This paper will deal primarily with the use of electric fields and uniaxial stress in studies of valence band mixing in single quantum wells. In the first section the

samples and experimental technique will be presented. Next a discussion of the effects of electric fields will be given. A section on uniaxial stress follows. Examples of how the two techniques have been used will be presented in these sections. The final section is a summary of the results of this study.

Samples and experimental technique

The samples used in this study were grown by molecular beam epitaxy (MBE). They consisted of a layer of n^+ GaAs grown on an n^+ GaAs substrate. Following this a layer of $\text{Al}_x\text{Ga}_{1-x}\text{As}$ with a thickness of from 500 to 10,000 Å was grown. This layer was usually undoped although in some instances the first few hundred angstroms were doped n^+ . One or more undoped GaAs quantum wells were then grown separated by $\text{Al}_x\text{Ga}_{1-x}\text{As}$ barriers with approximately 230 Å thickness. A layer of $\text{Al}_x\text{Ga}_{1-x}\text{As}$ with the same thickness as the first layer was grown on top of the wells. For these samples the aluminum composition was usually 30 per cent ($x=0.3$). The structure was capped with either a semitransparent layer of metal to form a Schottky barrier or a layer of p^+ GaAs to form a p - i - n diode. By changing the bias on the resultant diode, the electric field perpendicular to the quantum well could be varied. In some instances, the thickness of the $\text{Al}_x\text{Ga}_{1-x}\text{As}$ layers and number of quantum wells were chosen to form a leaky waveguide structure²¹ allowing illumination from the edge of the wafer. Compressive uniaxial stresses were applied to these samples by cleaving the wafers and mounting them in a stress apparatus similar to that diagrammed in Ref. 22. The stress was applied along a [110] axis which was perpendicular to a growth axis.

Excitonic transitions between the conduction and valence band subbands were studied using photocurrent and photoluminescence excitation spectroscopy. For these measurements the sample was mounted in a variable temperature cryostat. In the photocurrent measurements the sample was illuminated with the light from a grating monochromator using a tungsten lamp source. Illumination intensities were less than $10 \mu\text{Wcm}^{-2}$. A bias was applied to the sample and the photocurrent coming from the diode was collected as a function of wavelength to obtain a photocurrent spectrum. As long as the internal quantum efficiency of the diode is not a strong function of wavelength, the photocurrent spectrum is proportional to an absorption spectrum. For the excitation spectroscopy measurements, a Kr^+ -ion laser was used to pump an LD700 dye which was used to excite the sample optically. Power densities less than 500mWcm^{-2} were used. A 3/4-m spectrometer was set at the wavelength of the heavy hole emission from the quantum well, and the photoluminescence signal from the sample was detected as a function of excitation wavelength with a photomultiplier tube. Excellent agreement between the two techniques was obtained.

Figure 1 shows a sequence of photocurrent spectra taken on a sample with 80 Å wide quantum wells.¹⁸ Each spectrum was taken with a different applied bias which is given to the left of the spectrum. The width of the intrinsic region in this sample was approximately 2100 Å and the built-in voltage was 1.5 V. The four lowest energy peaks have been identified as h_1 , l_1 , h_{12} , and h_{13} (where h_1 and l_1 correspond to 1s ground states of excitonic transitions from the $n=1$ heavy or light hole valence subbands to the $n=1$ conduction subband, and h_{ij} is the excitonic transition from the $n=j$ heavy hole subband to the $n=i$ conduction subband). In this figure two features stand out. First, as the electric field in the well is increased, the exciton peaks Stark shift to longer wavelengths. Second, as the field is increased, the number of peaks visible in the spectrum increases. The new peaks which become visible are associated with forbidden transitions ($\Delta n \neq 0$). The perturbing field distorts the wavefunctions of the electrons and holes in the wells and changes the overlap of the wavefunctions. For h_1 and l_1 this should lead to a decrease in absorption coefficient,¹⁴ but, for forbidden transitions such as h_{12} , the field breaks the symmetry of the well and increases the absorption coefficient.

Figure 2 shows a plot of the energies of h_1 , l_1 , and h_{12} as a function of bias voltage. Backgrounds have been subtracted from the curves so that the energies will be approximately zero when the electric field in the well is zero. Also included in the figure are calculations of the energies of the excitons as a function of bias using the resonant tunneling technique of Ref. 15. In this figure we note that the Stark shifts of h_1 and l_1 are considerably larger than the shifts of h_{12} . This can actually be seen in Fig. 1. The reduced shift of h_{12} is due to a reduction in the shift of the $n=2$ heavy hole valence subband toward the valence band edge in comparison to the $n=1$ heavy and light hole subbands. Qualitatively, this difference follows from an argument based on a second order perturbation theory analysis of Stark shifts of the states in a one-dimensional quantum well.¹⁸ The calculations shown in Fig. 2 do predict a reduced shift for the $n=2$ heavy hole subband and, hence, for h_{12} . Figure 2 also shows that h_1 shifts more than l_1 . The fact that different excitons exhibit different shifts in an electric field can be used to cause crossings between exciton peaks.²³ This will be discussed next.

Figure 3 presents an excitation spectrum for a sample with 160 Å quantum wells. The depletion region was approximately 3100 Å wide and the built-in voltage was around 1.75 V. The spectrum was taken with the diode forward biased to flat band conditions (no electric field in the well). The l_1 peak and the high energy side of the h_1 peak are visible. Two additional peaks with considerably smaller amplitudes have been labelled $h_1^{(2x)}$ and $l_1^{(2x)}$. They correspond to the 2s and 2p states of the h_1 and l_1 excitons. (It will be shown below that both the s and the p excited states may be contributing to $h_1^{(2x)}$ so x represents either s or p.) This assignment is based on a comparison with previously published spectra and on agreement of the energy separations of $h_1^{(2x)}$ and $l_1^{(2x)}$ from h_1 and l_1 , respectively,

with calculated values (see for example Ref. 24,25). The peak h_{12} , which is also visible in Fig. 3 will be discussed below. Figure 4 is a sequence of excitation spectra for this sample taken in the energy range of the l_1 and $h_1^{(2x)}$ peaks. The bias voltage at which each spectrum was obtained is given beside the spectrum. For this well width the separation between l_1 and h_1 in a square well is less than the binding energy of h_1 , so, $h_1^{(2x)}$ appears at a higher energy than l_1 at zero electric field. As the field is increased, h_1 and, therefore, $h_1^{(2x)}$ shift to longer wavelength faster than l_1 and an anticrossing between $h_1^{(2x)}$ and l_1 occurs. This is clearly seen in Fig. 5 where the energies of $h_1^{(2x)}$ and l_1 are plotted as a function of bias. Also included in Fig. 5 are calculations of the energies in the effective mass approximation neglecting any mixing. The insert to Fig. 4 shows that fine structure actually becomes visible in the $h_1^{(2x)}$ peak as it crosses l_1 . This fine structure is attributed to the appearance of the 2p excited state of h_1 .²³ In a two dimensional system the reduction in symmetry splits the degeneracy between the 2s and 2p states of a hydrogenic exciton. The separations observed here are in agreement with calculations of the 2s and 2p splitting.^{26,27}

Quantum wells under uniaxial stress

In bulk GaAs uniaxial stress splits the degeneracy at $k=0$ between the heavy and light hole valence bands.²² Similarly, heavy and light hole valence subbands in a quantum well exhibit different shifts under a uniaxial stress. In contrast to bulk GaAs, the axis along which the stress is applied has a large effect on the results in a quantum well. Figure 6a is a calculation of the shifts of h_1 and l_1 for a compressive uniaxial stress applied along the [001] growth axis (perpendicular to the plane of the well). Figure 6b is a calculation for the stress applied along a [100] axis which is parallel to the plane of the quantum well. The calculations were done using a k.p theory⁴ and do not include any corrections for changes in the exciton binding energy as a function of stress. In both cases the exciton peaks shift to longer wavelength, but for an [001] stress the heavy hole peak shows the largest shift while for a [100] stress the change in energy of the light hole peak is greatest. This difference is due to the fact that for stress along [001] the strain and quantum confinement terms in the Hamiltonian can be simultaneously diagonalized, while for [100] stress they cannot be. In the first case, a strain produces essentially the same shifts as are observed for the heavy and light hole excitons in bulk GaAs. In the second case the strain causes a mixing between the excitons and different shifts are observed. The calculations in Fig. 6 indicate that the shifts of the excitons are dependent on the width of the quantum wells. For [001] stress, the shifts in h_1 are essentially width independent. The width dependence for l_1 is due to stress induced coupling with the split-off valence band. For a [100] stress, the shifts in l_1 and h_1 both depend on well width. This is a result of the fact that the stress induced mixing between heavy and light hole subbands which was mentioned above is a function of well width. Koteles et al.²⁰ recently reported the observation of a dependence of the shifts of h_1 and l_1 on well width for [100] stress. The calculations presented here are in excellent agreement with the results presented in Ref. 20. Calculations were also performed for a uniaxial

stress applied along a $[110]$ axis (which was the experimental configuration used in this study). The results were essentially the same as for Fig. 6b. The calculations also showed that higher energy heavy and light hole excitons exhibited nearly the same stress dependent shifts as h_1 and l_1 , respectively. From this we conclude that a uniaxial stress can be used to identify the symmetry of the valence band from which an exciton arises. For stress along the $[110]$ axis, a heavy hole exciton should exhibit a much smaller shift than a light hole exciton.

We have used these uniaxial stress results in combination with polarization dependent photocurrent measurements to identify a second example of mixing between heavy and light hole excitons in a GaAs quantum well.¹⁹ In Fig. 7 we give a set of photocurrent and photoluminescence excitation spectra for the same sample as was used in Fig. 3. The spectra were recorded in the wavelength range where the h_1 , l_1 and h_{12} peaks were expected to be seen. Each spectrum was again taken with a different electric field applied to the sample. The field is given to the left of each spectrum. The range of fields used here is much larger than that of Figs. 4 and 5. As the field in the well is increased, the peak labelled h_{12a} (which was seen in Fig. 3) grows in amplitude. A new peak, h_{12b} , also becomes visible and grows in amplitude until at 44 kV/cm four peaks of approximately the same intensity are visible in the spectrum. Calculations in the effective mass approximation have been carried out for this sample. The calculations indicate that in the presence of an electric field only the h_1 , l_1 and h_{12} excitons should have appreciable absorption coefficients for the wavelength range of Fig. 7. Every sample we have studied which had a well width greater than approximately 120 Å has exhibited two exciton peaks (h_{12a} and h_{12b}) in the energy range where h_{12} is expected to occur. For smaller well widths only a single h_{12} peak was observed as can be seen in Fig. 1. As the electric field increases further, the amplitude of h_{12a} decreases relative to the rest of the peaks until it is only a shoulder on the high energy side of l_1 . It should also be noted that when h_{12b} first becomes visible it coincides in energy with the continuum edge of l_1 , while at higher fields h_{12a} disappears at the approximate energy of the l_1 continuum.

To help determine the origin of the extra h_{12} peak, polarization and uniaxial stress dependent photocurrent measurements were made. The symmetries of the valence subbands at zone center are such that for light polarized perpendicular to the $[001]$ growth axis (XY polarized), transitions from the heavy and light hole subbands to the conduction subbands are both dipole allowed. For light polarized parallel to the growth axis (Z polarized), only light hole transitions should be seen.²¹ Polarization dependent measurements for a sample with 130 Å quantum wells imbedded in a waveguide are given in Fig. 8a. The exciton peaks are broader than in Fig. 7, because the measurements were made at a higher temperature. Nevertheless, h_1 , l_1 , h_{12a} and h_{12b} are all visible in the XY polarized spectra. In the Z polarization a small h_1 peak is seen; possibly due to XY polarized light scattered in from the face of the sample. A large l_1 peak is visible, but any structure that could be attributed to h_{12a} or h_{12b} is much smaller relative to l_1 than in the XY polarized spectrum. This allows us to conclude that the

oscillator strengths of h_{12a} and h_{12b} arise primarily from the heavy hole valence band. A compressive uniaxial stress was applied to the same sample along the [110] crystal axis. In agreement with Fig. 6b above, h_1 showed a small shift compared to l_1 . Fig. 8b gives photocurrent spectra for the sample with no applied stress and for a stress of about 1 kbar. The h_1 peaks have been aligned in Fig. 8b, therefore, we expect heavy hole excitons to show little or no shift while light hole excitons show a large shift. l_1 and h_{12a} both exhibit shifts greater than 2.25 meV while the shift in h_{12b} is less than 0.6 meV.

The polarization dependent measurements indicate that h_{12a} arises from the heavy hole valence band while the uniaxial stress indicates it is light hole in character. This contradiction is resolved by realizing that the polarization dependent measurements only give information about the part of the wavefunction contributing to absorption. It is clear from this that h_{12a} has a mixed heavy and light hole character and that the light hole component is not contributing to absorption. Since h_{12a} and h_{12b} both increase in amplitude with increasing field, and since they are in the energy range where h_{12} is expected to occur, they must be associated with the $n=2$ heavy hole valence subband. From the fact that h_{12b} first becomes visible at the l_1 continuum edge and that h_{12a} disappears at high fields at the energy of the l_1 continuum, we can associate the two peaks with the $n=1$ light hole valence subband. We conclude that the two peaks arise from a mixing between the $n=1$ light hole and $n=2$ heavy hole valence subbands. Strong mixing between these two subbands has been predicted for well widths in the range of 160 Å in Ref. 2. This would explain why only one h_{12} peak is seen in Fig. 1, since as the well width is decreased the subbands separate and mixing is reduced.² It would also account for the reduced amplitude of h_{12a} as the field is increased, because the subbands separate as the field is increased (Fig. 2) and mixing again decreases. In the high field limit, h_{12b} becomes the true h_{12} exciton. We speculate that this mixing takes the form of an interaction between an excited state of l_1 and the $1s$ ground state of h_{12} . The excited states have considerably smaller oscillator strengths than the ground states but would become visible when mixing with h_{12} occurred. Recent work by Chan⁶ suggests that such mixing should occur between the p-like excited state of l_1 and the s-like states of h_{12} .

Summary

We have shown that in the presence of an electric field forbidden excitons ($\Delta n \neq 0$) become visible. Also, the excitons show a Stark shift in the field, and, because different excitons exhibit different shifts, the energy separations of the excitons change. The latter fact allowed us to observe an anticrossing between the l_1 and $h_1^{(2x)}$ exciton peaks. In contrast to bulk GaAs, the axis along which a uniaxial stress is applied has a large effect on the relative shifts of the heavy and light hole excitons. If the stress is applied along the growth axis, h_1 and l_1 move closer together. Stress perpendicular to this axis causes h_1 and l_1 to separate. We also found that the symmetry of the valence subband from which an exciton arises can be identified by applying a uniaxial stress. A uniaxial stress was used in con-

junction with electric field and polarization dependent measurements to identify an example of valence band mixing in quantum wells with widths greater than approximately 120Å. An extra exciton peak which was observed in the energy range where the h_{12} exciton is predicted to occur was shown to have a mixed heavy and light hole character. It was attributed to mixing between the $n=2$ heavy and $n=1$ light hole valence subbands.

Acknowledgments

The authors acknowledge J. R. Kirtley, E. E. Mendez, K. v. Klitzing, K. Ploog, L. L. Chang, and L. Esaki for valuable discussions during the course of this work.

References

- 1.) M. Altarelli, Phys. Rev. B **28**, 842 (1983).
- 2.) J. N. Schulman and Y. C. Chang, Phys. Rev. B **31**, 2056 (1985).
- 3.) D. Ninno, M. A. Gell, and M. Jaros, J. Phys. C **19**, 3845 (1986).
- 4.) C. Mailhot and D. L. Smith, Phys. Rev. B **33**, 8360 (1986).
- 5.) G. D. Sanders and Y. C. Chang, Phys. Rev. B **32**, 5517 (1985).
- 6.) K. S. Chan, J. Phys. C **19** L125 (1986).
- 7.) D. A. Broide and L. J. Sham, Phys. Rev. B **34** 3917 (1986).
- 8.) R. C. Miller, A. C. Gossard, G. D. Sanders, Y. C. Chang, and J. N. Schulman, Phys. Rev. B **32**, 8452 (1985).
- 9.) J. N. Schulman and T. C. McGill, Phys. Rev. B **19**, 6341 (1979).
- 10.) M. Jaros and K. B. Wong, J. Phys. C **17**, L765 (1984).
- 11.) D. J. Wolford, T. F. Kuech, J. A. Bradley, M. A. Gell, D. Ninno, and M. Jaros, J. Vac. Sci. Technol. B **4**, 1043 (1986).
- 12.) J. C. Maan, G. Belle, A. Fasolino, M. Altarelli, and K. Ploog, Phys. Rev. B **30**, 2253 (1984).
- 13.) D. C. Rogers, J. Singleton, R. J. Nicholas, C. T. Foxon, and K. Woodbridge, Phys. Rev. B **34**, 4002 (1986).
- 14.) E. E. Mendez, G. Bastard, L. L. Chang, L. Esaki, H. Morkoç, and R. Fischer, Phys. Rev. B **26**, 7101 (1982).
- 15.) D. A. B. Miller, D. S. Chemla, T. C. Damen, A. C. Gossard, W. Weigmann, T. H. Wood, and C. A. Burrus, Phys. Rev. B **32**, 1043 (1985).
- 16.) H. -J. Polland, L. Schultheis, J. Kuhl, E. O. Göbel, and C. W. Tu, Phys. Rev. Lett. **55**, 2610 (1985).
- 17.) L. Viña, E. E. Mendez, W. I. Wang, L. L. Chang, and L. Esaki, Accepted for publication in J. Phys. C: Solid State.
- 18.) R. T. Collins, K. v. Klitzing, and K. Ploog, Phys. Rev. B **33**, 4378 (1986).
- 19.) R. T. Collins, L. Viña, W. I. Wang, L. L. Chang, L. Esaki, K. v. Klitzing, and K. Ploog, in Proceedings of the 18th International Conference on the Physics of Semiconductors, Stockholm, Sweden, 1986 (to be published).
- 20.) Emil S. Koteles, C. Jagannath, Johnson Lee, Y. J. Chen, B. S. Elman, and J. Y. Chi, in Proceedings of the 18th International Conference on the Physics of Semiconductors, Stockholm, Sweden, 1986 (to be published).

- 21.) J. S. Weiner, D. S. Chemla, D. A. B. Miller, H. A. Haus, A. C. Gossard, W. Wiegmann, and C. A. Burrus, *Appl. Phys. Lett.* **47**, 664 (1985).
- 22.) F. H. Pollak and M. Cardona, *Phys. Rev.* **172**, 816 (1968).
- 23.) L. Viña, R. T. Collins, E. E. Mendez, and W. I. Wang, *Phys. Rev. Lett.*, accepted for publication.
- 24.) R. C. Miller, D. A. Kleinman, W. T. Tsang, and A. C. Gossard, *Phys. Rev. B* **24**, 1134 (1981).
- 25.) P. Dawson, K. J. Moore, G. Duggan, H. I. Ralph and C. T. B. Foxon, *Phys. Rev. B* **34**, 6007 (1986).
- 26.) Y. Shinozuka and M. Matsuura, *Phys. Rev. B* **28**, 4878 (1984).
- 27.) R. L. Greene, K. K. Bajaj, and D. E. Phelps, *Phys. Rev. B* **29**, 1807 (1984).

Figures

Fig. 1. Photocurrent spectra for an 80 \AA wide quantum well at different bias voltages. The baselines of the spectra have been offset for clarity.

Fig. 2. Energies of the three lowest energy exciton peaks in Fig. 1 as a function of bias. The energies have been offset by approximately the flat band exciton energies. The solid lines are calculated values using the envelope function approximation and assuming binding energies between 5.0 and 9.0 meV .

Fig. 3. A Photoluminescence excitation spectrum for a 160 \AA quantum well. The electric field in the well is less than 3 kV/cm .

Fig. 4. Excitation spectra for the sample of Fig. 3 in the spectral range of the l_1 and $h_1^{(2x)}$ exciton peaks. The bias voltage at which each spectrum was obtained is given beside the spectra. The insert follows $h_1^{(2x)}$ through bias voltages at which a splitting between $2s$ and $2p$ states is resolved. The dashed lines are a visual aid to help follow the two peaks.

Fig. 5. Energies of the l_1 and $h_1^{(2x)}$ peaks in Fig. 4 as a function of electric field. The solid and dashed lines are calculations of the Stark shifts of the peaks in the effective mass approximation neglecting changes in the binding energy and excitonic coupling. The error bar gives the uncertainty in the field.

Fig. 6. Calculated shifts of the h_1 and l_1 excitons as a function of uniaxial stress (X) for the stress applied along the a) $[001]$ growth axis and b) along a $[100]$ axis which is perpendicular to the growth axis. Two well widths were used (40 \AA and 220 \AA). The Aluminum composition was 30 per cent.

Fig. 7. Photocurrent (dashed) and photoluminescence excitation (solid) spectra for the 160 Å quantum well sample of Fig. 3 as a function of electric field. The field is given beside the spectra. The baselines of the spectra have been offset for clarity.

Fig. 8. a) Polarization dependent photocurrent spectra for a 130 Å quantum well imbedded in an $\text{Al}_x\text{Ga}_{1-x}\text{As}$ waveguide. b) Uniaxial stress dependent photocurrent spectra for the same sample. The h_1 peaks have been aligned. In both a and b the electric fields in the well are given beside the spectra.

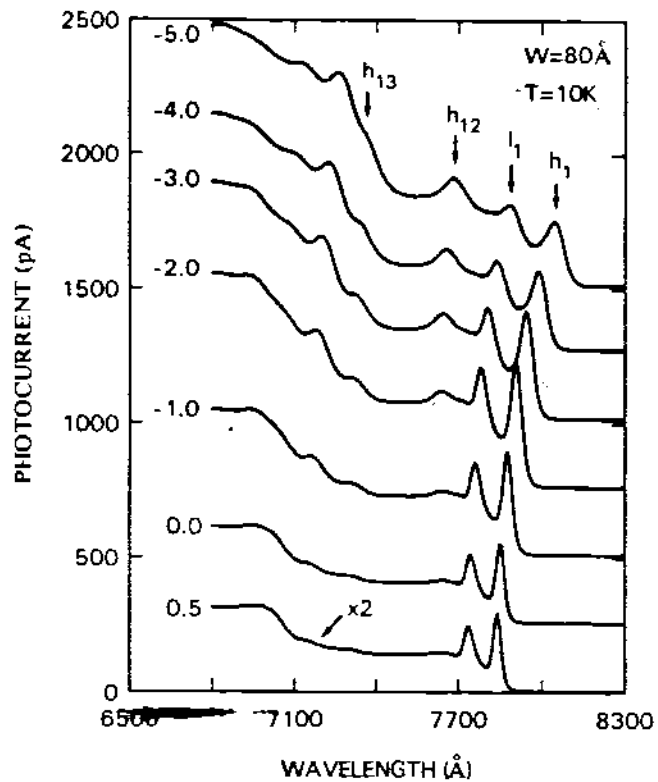


Fig 1

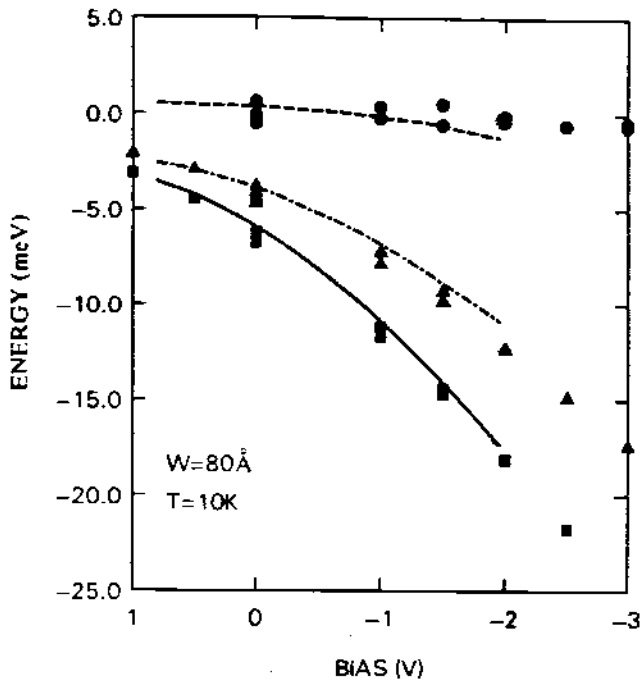


Fig 2

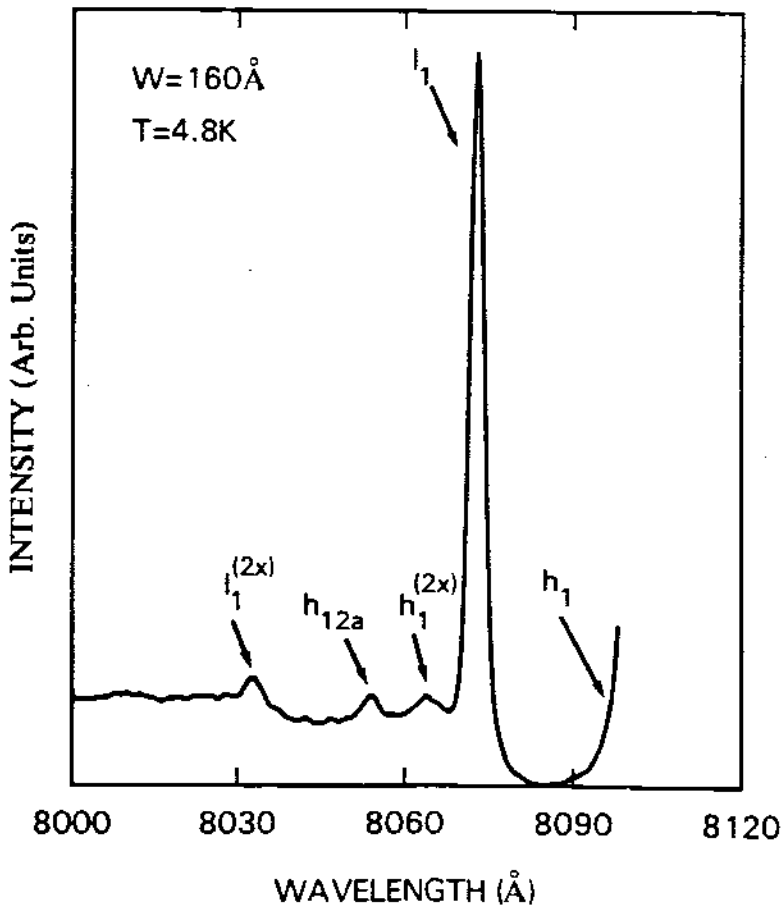


Fig 3

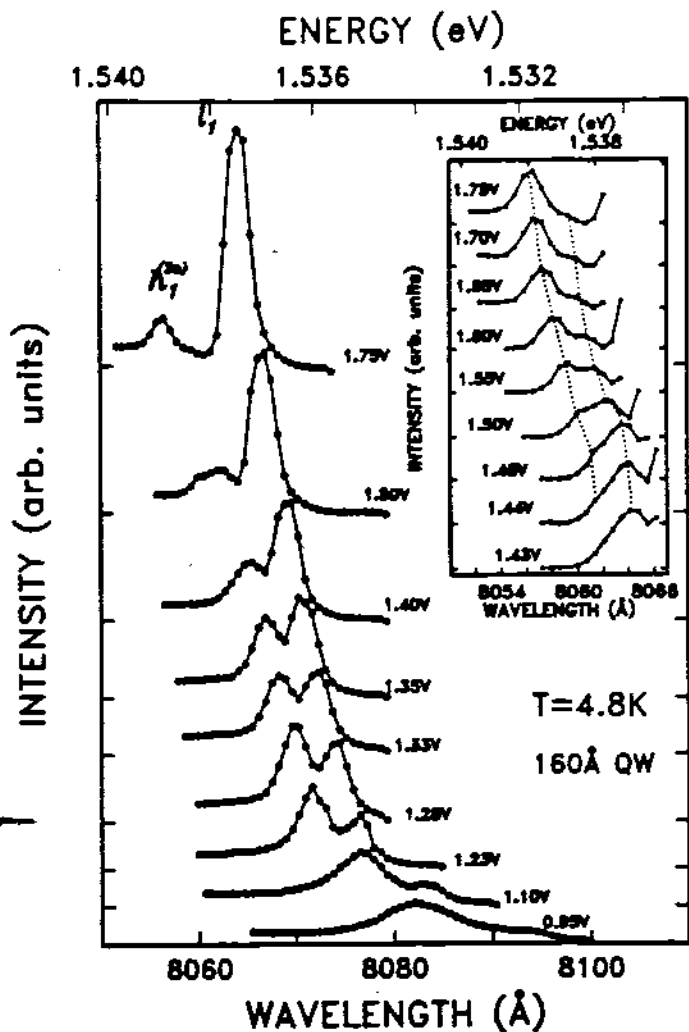


Fig 4

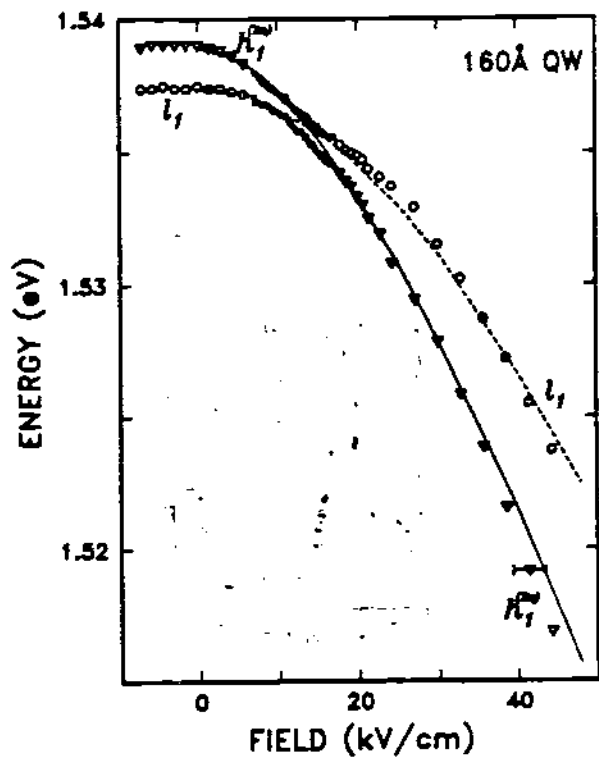


Fig 5

Fig. 6 a, b

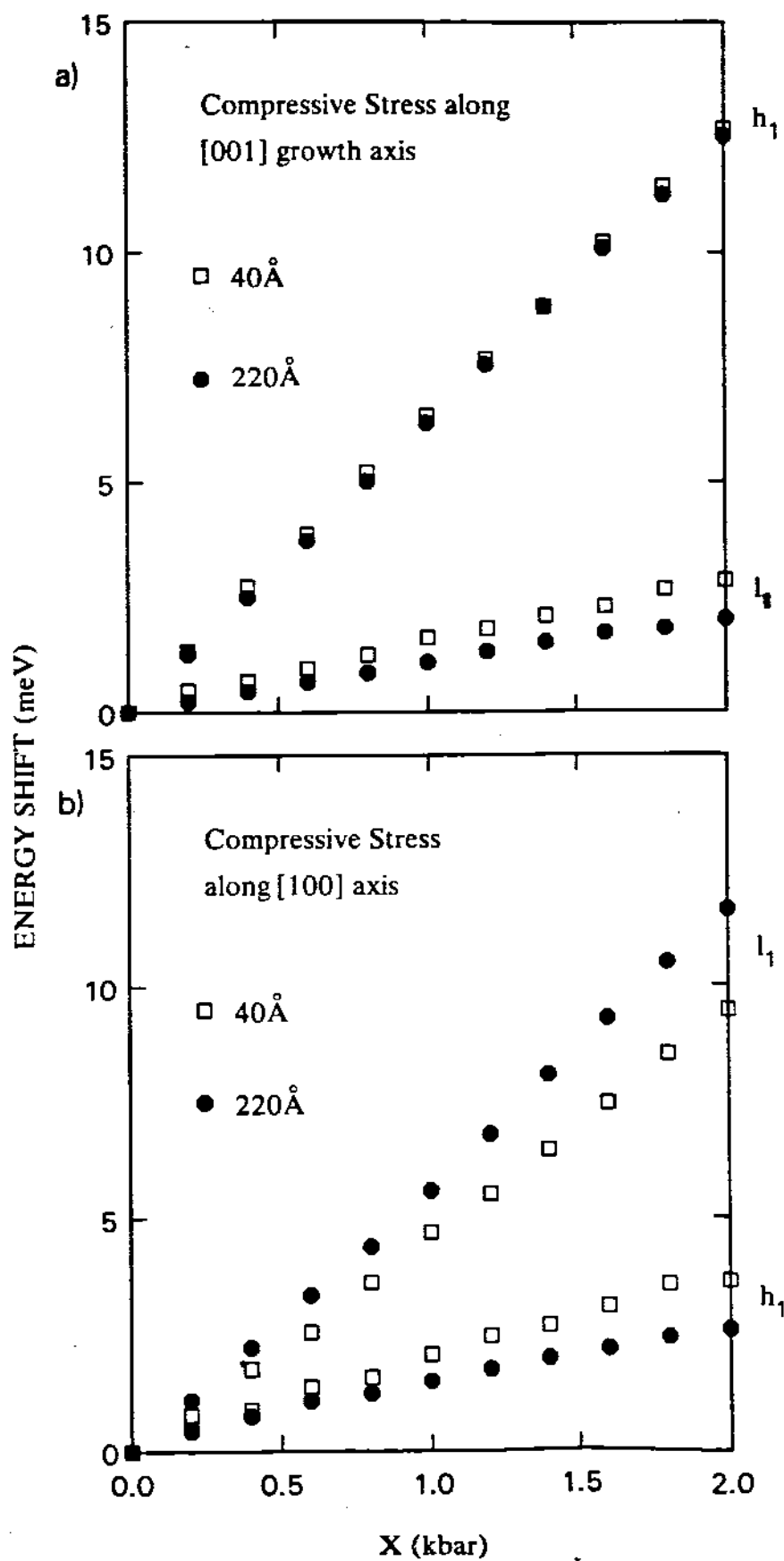
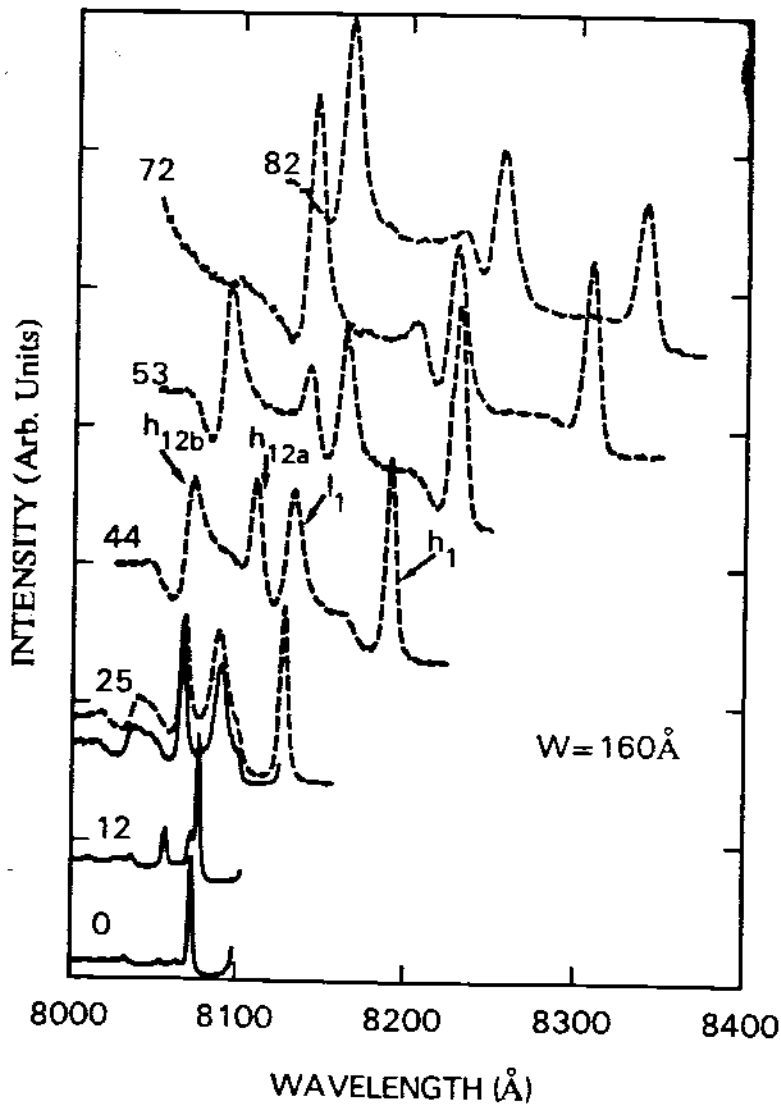


Fig 7.



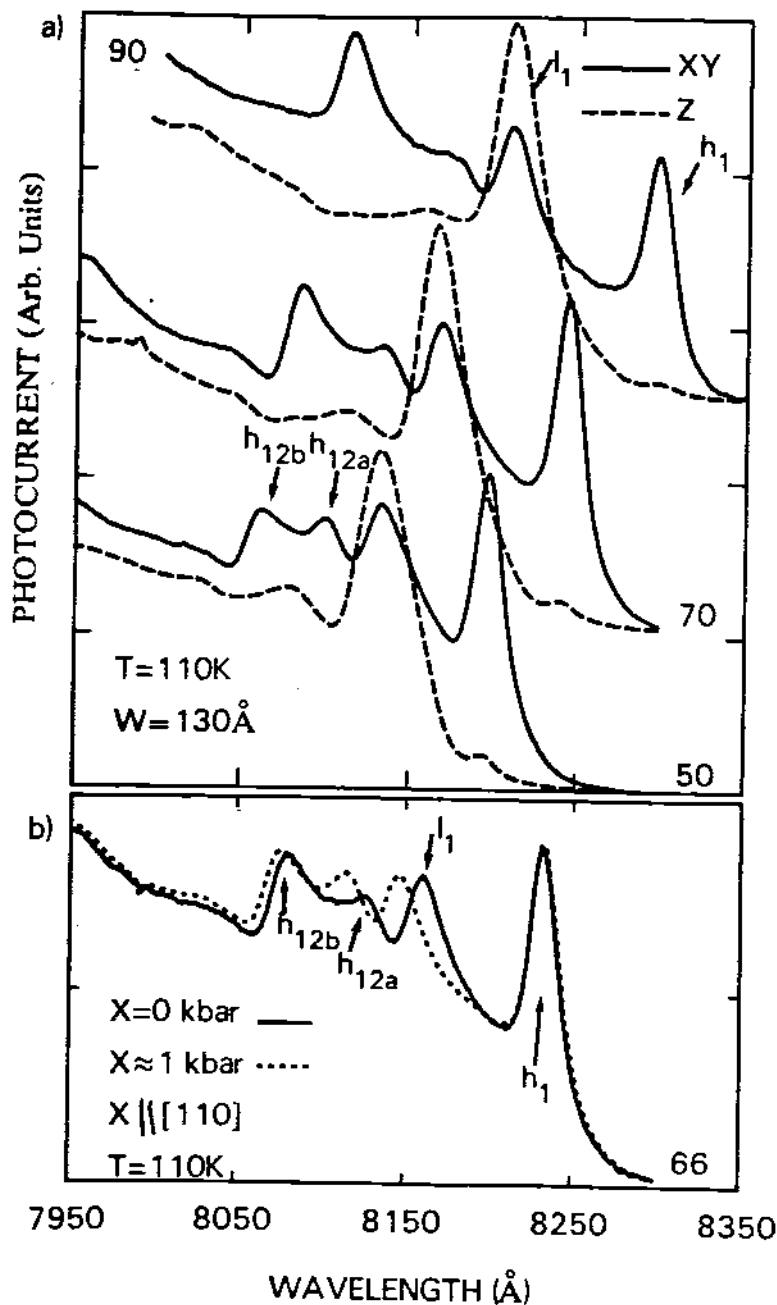


Fig 8 a, b